Finite Element Analysis of RC Beams with Rectangular Web Openings in Flexure Zone Strengthened with CFRP

1Ali Gamal Ali AbdEl-shafy, 2Mohamed Mahmoud Ahmed Mohamed, 3Fawzy Mohamed Ahmed El-Beheiry, 4Mohamed Ali Mohamed SaadEl-deen
1Professor, 2Professor, 3Associate Professor, 4Assistant Lecturer
Assuit faculty of engineering

***Abstract* - This paper presents a nonlinear Finite Element Analysis (FEA) that has been carried out to study the behavior of fiber reinforced polymer (FRP) strengthened reinforced concrete (RC) beams containing large rectangular web openings in the flexure zone. Studied parameters were type of loading and opening size. Eleven RC beams categorized into two different groups were adoptable in FE model software using ANSYS V14. The analysis results compared with five experimental beams had been done by Almusallam et al. 2018 [1]. In the first group, eight beams were tested under center-point loading. They comprised of one reference solid beam and seven beams with large rectangular web opening with different dimensions located at the maximum-moment region. Out of the seven beams with openings, four beams were unstrengthened and the other three were strengthened with carbon fiber reinforced polymer (CFRP) sheets. In the second group, three beams were tested under four-point bending. They comprised of one reference solid beam (without opening) and two beams with large rectangular web opening in the pure flexure zone. Out of the two beams with openings, one specimen was unstrengthened and the other one was strengthened with (CFRP) sheets. The failure loads, crack pattern and mode of failure were analyzed here in this study.**

***keywords* - Finite element analysis (FEA), openings, flexural strengthening, FRP.**

I. INTRODUCTION

The web openings in reinforced concrete (RC) beams have important applications in practice as they provide convenient passages of electrical and mechanical conduits. These openings accommodate vital building services that may include electricity, air conditioning, water supply, computer and telecommunication network. The web openings in RC beams may be of different shapes such as rectangular, circular, trapezoidal, diamond, and many other shapes. The presence of a rectangular opening leads to a decrease in both cracking and ultimate strengths as well as stiffness of RC beams. The amount of reduction is significantly affected by opening proximity to support, opening height, and opening length, but is slightly affected by tension and compression reinforcement ratios *(Arafa Mahmoud Ahmed 2010)* [2]. Many researchers have used the terms "small" and "large" openings for their classification without any clear distinction. *Mansur, 1998* [3] suggested the criteria to classify the size of openings. Author classified the web opening as small if $\ell_o \leq h_c$ where ℓ_o is the length of the opening and h_c is the larger of h_b and h_t; where h_b and h_t are the depths of bottom and top chords, respectively (see **Fig. 6**). For large opening, $\ell_o > h_c$, the post-construction creation of an opening in the web of RC beams reduces the web cross-section and consequently reduces the flexural stiffness and shear capacity and increases the beam deflection at service load *)Mansur, MA Tan, KH Wei, 1999)* [4]. For post-constructed openings in the existing RC beams, retrofitting of beams is needed. Fiber-reinforced polymer (FRP) is currently emerging as a popular option to repair and strengthen reinforced concrete structures.

The influence of FRP laminates on the response of solid RC beams under flexure and shear has been widely studied. However, the research on the use of FRP laminates in the strengthening of RC beams with opening is limited)*Mansur, MA Tan, KH Wei, 1999* [4]*; Abdalla et al., 2003* [5]*; El Maaddawy & Sherif, 2009* [6]*; Pimanmas, 2010* [7]*; Hawileh et al., 2012* [8]*; Hassan et al., 2017* [9]*; Nie et al., 2017* [10]). Some of these studies were performed using experiments and validated with nonlinear finite element (FE) analysis (*Pimanmas, 2010* [7]*; Hawileh et al., 2012* [8]). Even though some studies have been published on FRP-upgraded RC beams with web openings located in shear zones, research on FRP-graded RC beams with web openings in flexure zones is very limited. This highlights the need for more research in this area.

Almusallam et al. 2018 [1] studied experimentally the performance of CFRP-strengthened RC beams having rectangular opening in flexure zone. Seven RC beams were tested up to failure under center-point loading/four-point bending loading. It was reported that large opening in flexure zone increases cracking and deflection and reduces the load capacity and stiffness. A strengthening configuration was designed once the flexural tests for the unstrengthened specimens with and without openings were done and the failure patterns established.

The goal of this study is to examine numerically the influence of rectangular web opening in the flexure zone on the response of unstrengthened and strengthened RC beams and compare the analysis results with available experimental data had

been done by *Almusallam et al. 2018* [1]. Studied parameters included type of loading and opening size. Eleven RC beams were tested up to failure. Two loading types and four different opening sizes were investigated.

II. FINITE ELEMENT MODELING

A three dimensional finite-element program 'ANSYS V14' was used for modeling reinforced concrete beams with the dimensions and properties corresponding to beams experimentally tested by (Tarek and Yousef). In the analysis, appropriate material models were employed to represent the behavior of concrete, the steel reinforcement, the steel plates and CFRP laminates.

Concrete

A solid element, Solid65, is used to model the concrete in ANSYS. The solid element has eight nodes with three transitional degrees of freedom at each node – translations in the nodal x-, y- and z-directions. In addition, the element is capable of simulating plastic deformation, cracking in three orthogonal directions, and crushing. The geometry and node locations for this element type are shown in **Fig. 1**.

Steel Reinforcement

A Link180 element was used to model steel reinforcement. The element is a uniaxial tension-compression element with three degrees of freedom at each node: translations in the nodal x, y, and z directions. Plasticity, creep, rotation, large deflection, and large strain capabilities are included. This element is shown in **Fig. 2**. A perfect bond between the concrete and steel reinforcement considered. However, in the present study the steel reinforcing was connected between nodes of each adjacent concrete solid element, so the two materials shared the same nodes. The same approach was adopted for FRP composites. Steel reinforcement in the experimental beams was constructed with typical steel reinforcing bars. Elastic modulus and yield stress for the steel reinforcement used in this FEM study follow the design material properties used for the experimental investigation (*Almusallam et al. 2018* [1]). The steel for the finite element models is assumed to be an elastic-perfectly plastic material and identical in tension and compression.

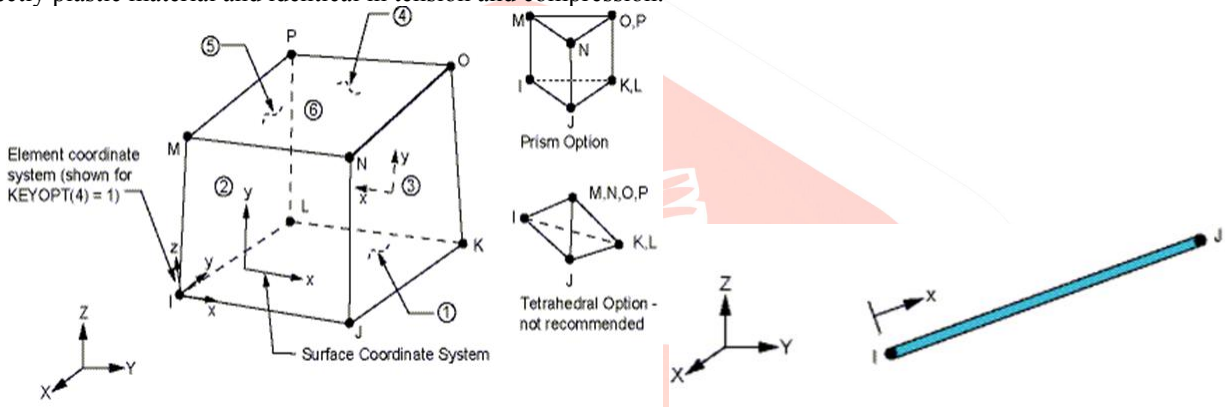

Fig. 1. Solid65 geometry – 3-D reinforced concrete solid **Fig. 2**. Link180 geometry – 3-D spar

Steel Plates

Steel plates were added at support and loading locations in the finite element models (as in the actual beams) in order to avoid stress concentration problems. An elastic modulus equals to 200,000 N/mm2 and Poisson's ratio of 0.3 were used for the plates. The steel plates were assumed to be linear elastic materials. A Solid 45 element was used to model steel plates. The element is defined with eight nodes having three degrees of freedom at each node translations in the nodal x, y, and z directions. The geometry and node locations for this element type are shown in **Fig. 3**.

FRP Laminates

The FRP composites are orthotropic materials; that is, their properties are not the same in all directions, **Fig. 4** shows a schematic of FRP composites. A layered solid element, Solid 185, was used to model the FRP composites. The element allows for up 100 different material layers with different orientations and orthotropic material properties in each layer. The element has three degrees of freedom at each node and translations in the nodal x, y, and z directions. The high strength of the epoxy used to attach FRP sheets, as in the experimental beams supported the perfect bond assumption. The geometry, node locations, and the coordinate system are shown in **Fig. 5**.

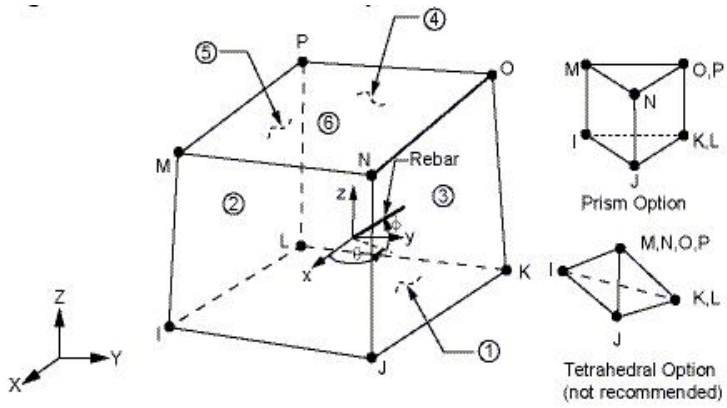

Fig. 3. Solid45 geometry – 3-D solid

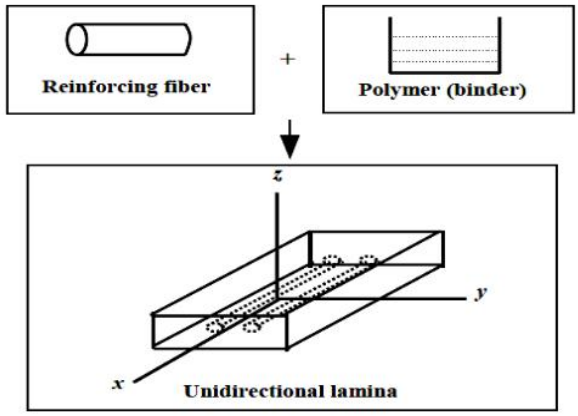

Fig. 4. Schematic of FRP composites

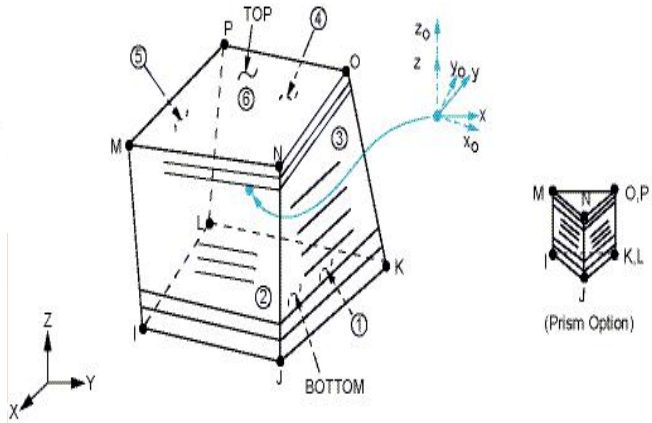

Fig. 5. Solid185 geometry – 3-D layered structural solid

III. PROGRAM OF STUDY

The numerical analysis was carried out on eleven reinforced concrete beams of 2800 mm span with section dimensions of 200 x 450 mm. Details of the analyzed beams are presented in **Table 1**. Beams were categorized into two different groups. In the first group, eight beams were tested under center-point loading (CPL). They comprised of one reference solid beam (without opening), one beam with mid-span rectangular opening of 225 mm depth and 225 mm length, two beams with mid-span rectangular opening of 225 mm depth and 450 mm length, two beams with mid-span rectangular opening of 225 mm depth and 675 mm length and two beams with mid-span rectangular opening of 225 mm depth and 900 mm length, see **Table 1**. Out of the seven beams with openings, four specimens were unstrengthened and the other three were strengthened with two layers of externally bonded CFRP sheets. In the second group, three unstrengthened beams were tested under four-point bending (4PB). They included one solid reference specimen (without opening) and the other two beams were with a large rectangular web opening of 225 mm depth and 450 mm length in the pure flexure zone. Out of these two beams with openings, one of them was unstrengthened and the other one was strengthened with two layers of externally bonded CFRP sheets.

Details of unstrengthened specimens are given in **Figs. 6** and **7** for beams with center-point loading and 4-point bending, respectively. For beams with openings, a single rectangular opening was constructed at mid-span and it was located symmetrically, as shown in **Figs. 6** and **7**. U-stirrups were provided in the bottom and top chords of the opening, thus representing the creation of the opening on site by cutting concrete and steel stirrups in existing beams. **Table 2** illustrates the material properties of concrete, steel and CFRP laminates used in the analysis.

As shown in **Fig. 8**, the scheme used in strengthening comprised of applying two layers of CFRP sheets in the designated patterns. CFRP strips of 112.5 mm width were applied to the bottom and top chords of the beam first, with the primary fibers oriented longitudinally. The strips were applied on both sides of RC beams, as shown in **Fig. 8a**. On top of these strips, the second layer of CFRP was applied with the pattern shown in **Fig. 8b**. The second layer comprised of four pieces of CFRP sheets with fibers oriented vertically, which were applied separately to the top and bottom chords, and on both sides of the opening. It should be noted that the chord above the opening and the two sides were wrapped using a U-shape wrap; whereas, the chord below the opening was fully wrapped.

Only quarter of the beam has been modeled to take the advantage of symmetry in ANSYS. The mesh was taken square to obtain good results; it was taken 25 x 25 x 25 mm as shown in **Fig. 9**. The command merge items merge separate entities that have the same location. These items will then be merged into single entities. Caution must be taken when merging entities in a model that has already been meshed because the order in which merging occurs is significant. Displacement boundary conditions are needed to constrain the model to get a unique solution. The model being used is symmetric about two planes. Nodes defining a vertical plane through the beam cross-section center define a plane of symmetry. To model the symmetry,

nodes on this plane must be constrained in the perpendicular direction. These nodes, therefore, have a degree of freedom constraint UX = 0. Second, all nodes selected at Z = 0 define another plane of symmetry. These nodes were given the constraint UZ = 0. The support was modeled in such a way that a roller was created. A single line of nodes on the plate were given constraint in the UY, and UZ directions, applied as constant values of 0. By doing this, the beam will be allowed to rotate at the support. In this study the total load applied was divided into a series of load increments (or) load steps. Newton–Raphson equilibrium iterations provide convergence at the end of each load increment within tolerance limits. The automatic time stepping in the ANSYS program predicts and controls load step sizes for which the maximum and minimum load step sizes are required. Finite element mesh, boundary condition, loading regions, steel reinforcement and FRP composite for a quarter beam model of all beams are shown in **Figs. 10**, **11** and **12**.

Group	Beam ID.	Opening size (mm)		ℓ_o / h_c	Type of loading	CFRP Strengthening
		h_o	ℓ_o			
A	**BU-N-CPL**	No opening		0	CPL	Unstrengthenend
	BU-2.0-CPL	225	225	2.0	CPL	Unstrengthenend
	BU-4.0-CPL	225	450	4.0	CPL	Unstrengthenend
	BS-4.0-CPL	225	450	4.0	CPL	Strengthened
	BU-6.0-CPL	225	675	6.0	CPL	Unstrengthenend
	BS-6.0-CPL	225	675	6.0	CPL	Strengthened
	BU-8.0-CPL	225	900	8.0	CPL	Unstrengthenend
	BS-8.0-CPL	225	900	8.0	CPL	Strengthened
B	**BU-N-4PB**	No opening		0	4PB	Unstrengthenend
	BU-4.0-4PB	225	450	4.0	4PB	Unstrengthenend
	BS-4.0-4PB	225	450	4.0	4PB	Strengthened

Table 1. Details of the analyzed beams

Where; **B**old samples carried out experimentally, ho: height of the opening, ℓ_o: length of the opening, hc: larger depth of top and bottom chords of the opening, CPL: center-point loading, 4PB: four-point bending.

Property	Units	Value	
Concrete			
Modulus of elasticity	GPa	20	
Uniaxial compressive strength	MPa	50	
Steel rebars		*Mild*	*H.T.*
Modulus of elasticity	GPa	200	
Yield stress	MPa	540	575
Plastic strain to failure	%	11.7	11.7
CFRP laminates			
Thickness per layer	mm	1.0	
Longitudinal tensile strength	MPa	834	
Transverse tensile strength	MPa	83.4	
Modulus of elasticity in long. dir.	GPa	82	
Modulus of elasticity in transverse dir.	GPa	3.6	

Table 2. CFRP material properties used in the FE modeling

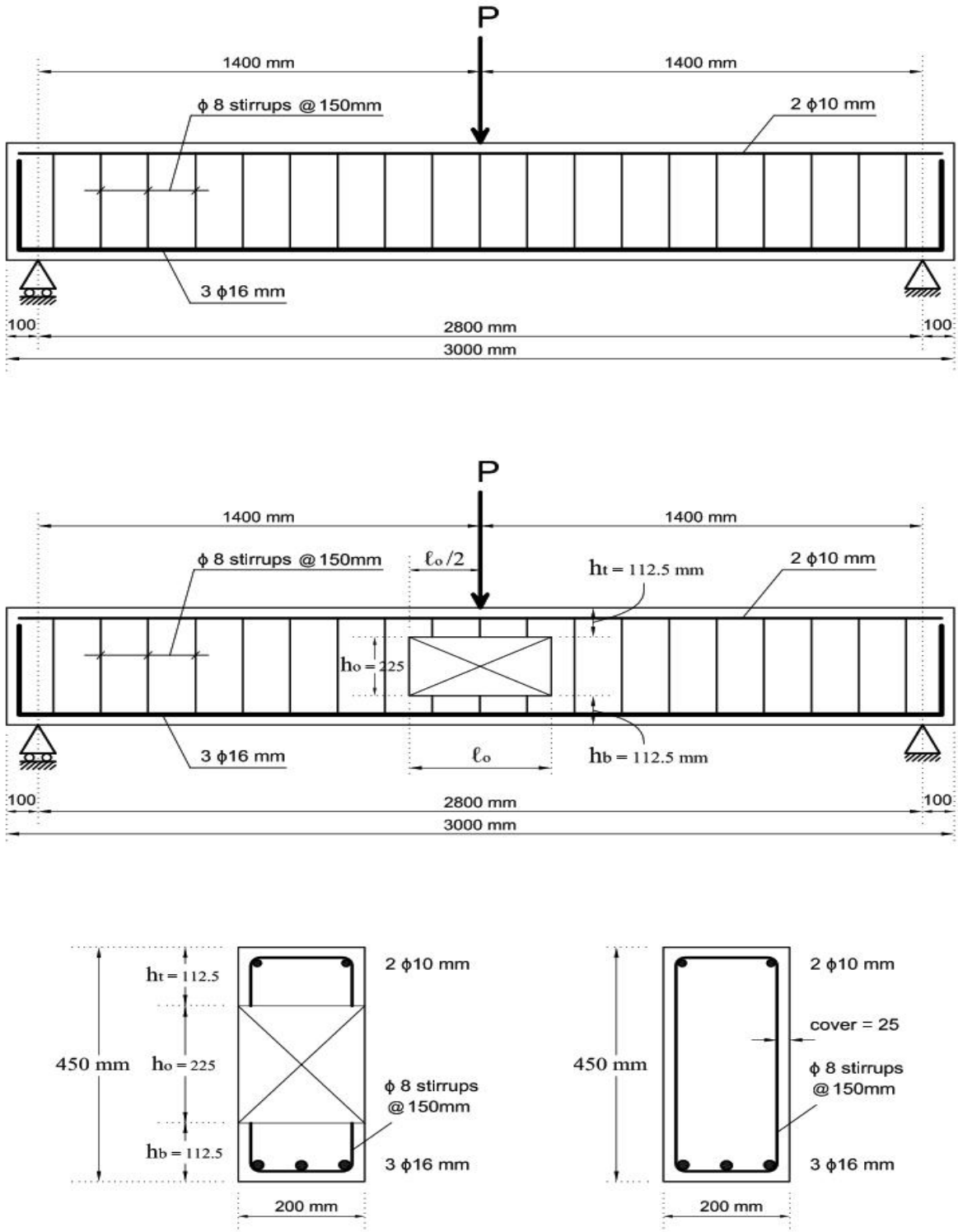

Fig. 6. Details of unstrengthened beams with center-point loading: **(a)** elevation of beam without opening, **(b)** elevation of beam with an opening, **(c)** beam section within solid parts, **(d)** beam section within opening location.

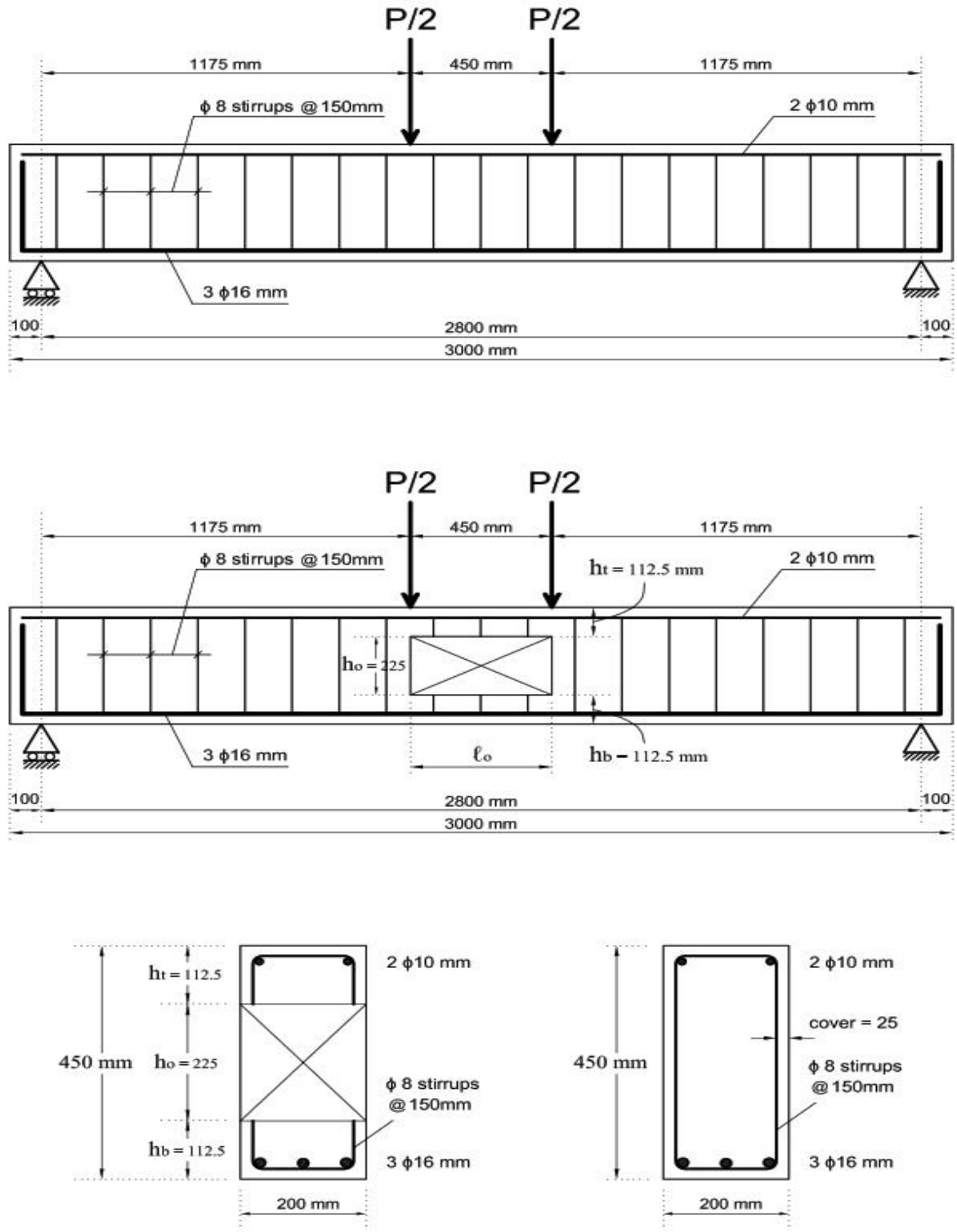

Fig. 7. Details of unstrengthened beams with 4-point bending: **(a)** elevation of beam without opening, **(b)** elevation of beam with an opening, **(c)** beam section within solid parts, **(d)** beam section within opening location.

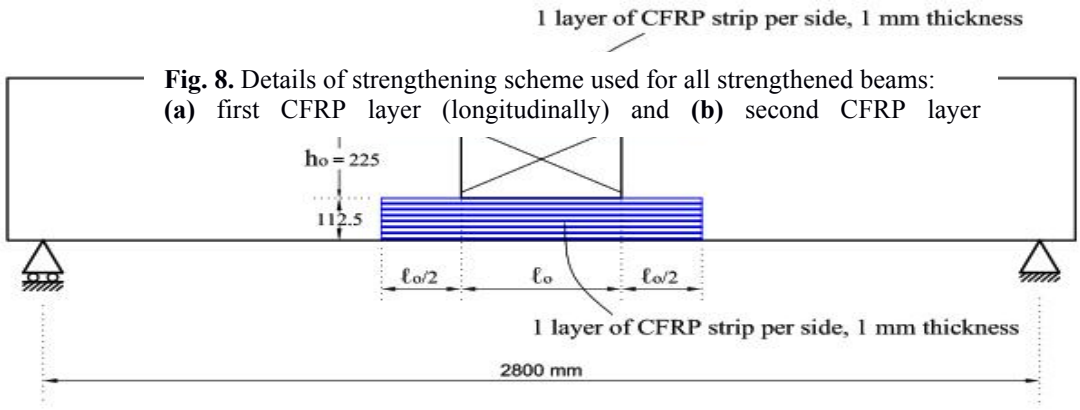

Fig. 8. Details of strengthening scheme used for all strengthened beams: **(a)** first CFRP layer (longitudinally) and **(b)** second CFRP layer

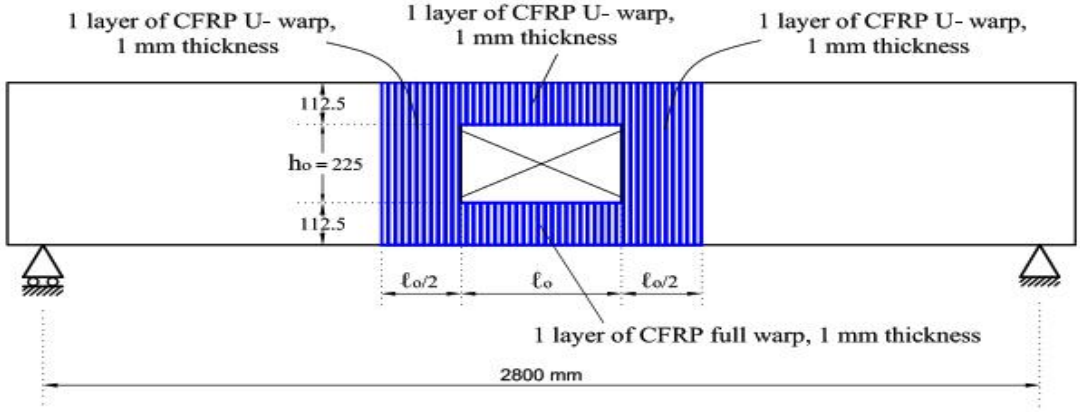

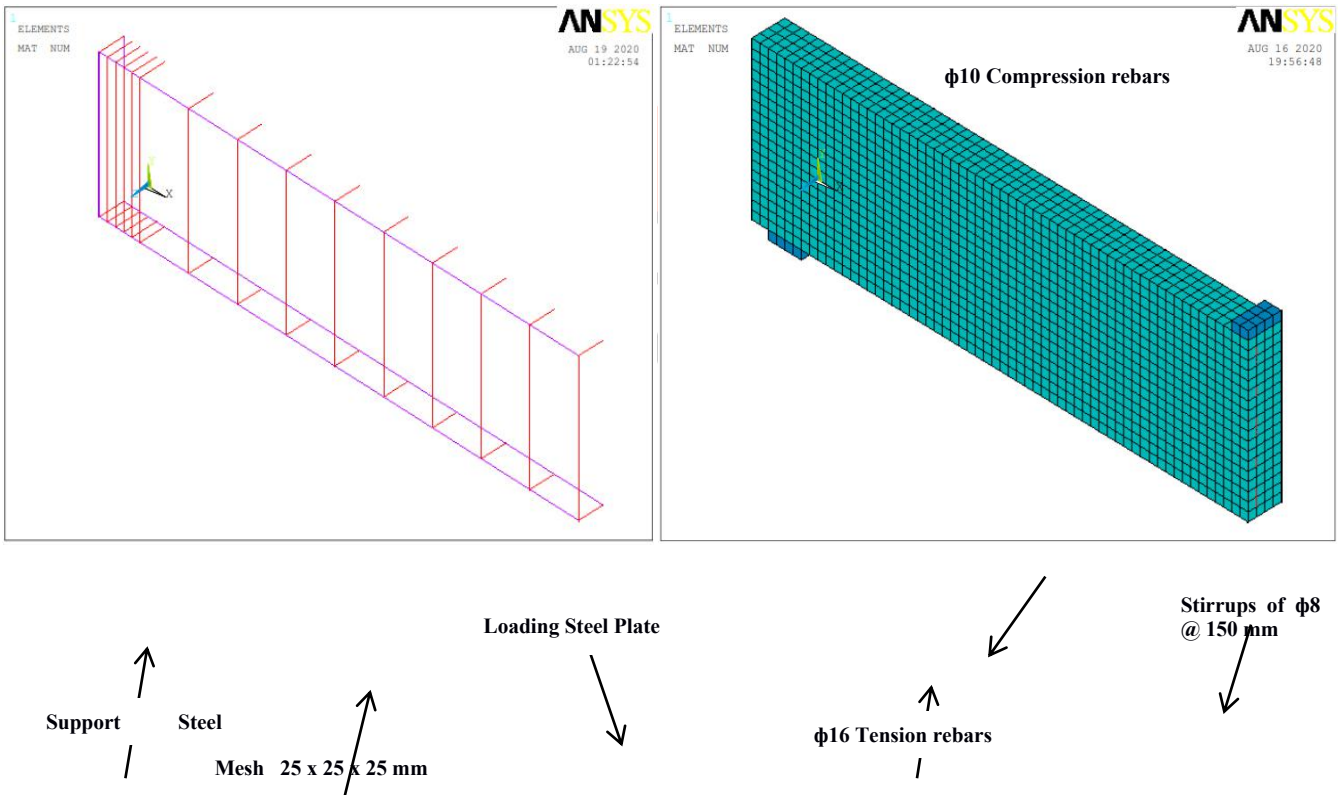

Fig. 9. Mesh of a quarter beam model of all

Fig. 10. FE model for one-quarter of beams – Steel

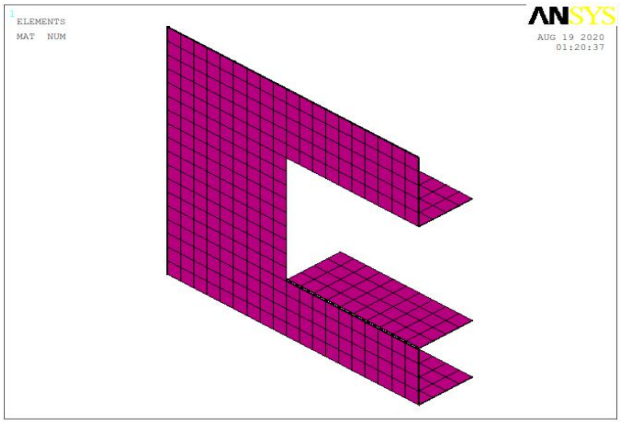

Fig. 11. FE model for one-quarter of beams –2nd CF

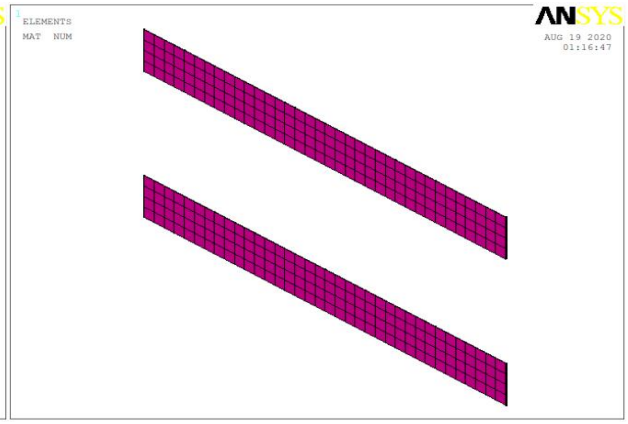

Fig. 12. FE model for one-quarter of beams – 1st CFRP layer

IV. Verification of Finite Element Analysis

Test results of the five rectangular reinforced concrete (RC) beams were employed for the verification of the numerical analysis and the experimental results that obtained from *Almusallam et al. 2018* [1]. Details of this beams specimens are summarized in **Table 1** as Bold samples. **Fig. 13** displays the modes of failure for the tested five beams, obtained from the experimental work and then using ANSYS program at the end of the analysis time. The modes of failure from ANSYS in this figure are shown using contours of maximum principal strains at the mid-surface. It is noticed from this figure that the modes of failure observed in the results of numerical analysis are either similar or almost identical to the ones determined experimentally. **Fig. 14** depicts

a comparison between the experimental and numerical variation of applied load versus mid-span deflection of RC beams for the five tested specimens. The figure shows good agreement between the numerical and experimental load–deflection curves and especially the peak loads for all test specimens. **Table 3** enlists the comparison details in terms of load-deflection characterist

Table 3. Comparison of experimental and FE load-deflection characteristics for the five tested beams.

Beam ID.	Results	P_y (KN)	P_u (KN)	Δ_y (mm)	Δ_u (mm)	Failure mode
BU-N-CPL	EXP	180	217	7.5	76.9	Y-CC
	FE	173.3	212.8	6.9	81.2	Y-CC
	EXP/FE	1.04	1.02	1.08	0.95	
BU-4.0-CPL	EXP	NY	181	NY	7	SF-TC
	FE	NY	187.7	NY	7.2	SF-TC
	EXP/FE	--	0.96	--	0.97	
BS-4.0-CPL	EXP	NY	193	NY	8.6	DB-SF-TC
	FE	NY	204.8	NY	8.8	DB-SF-TC
	EXP/FE	--	0.94	--	0.98	
BU-N-4PB	EXP	208	239	9.4	85.4	Y-CC
	FE	220	236	9.6	79.9	Y-CC
	EXP/FE	0.95	1.01	0.98	1.07	
BU-4.0-4PB	EXP	215	244	8.9	34.2	Y-CC
	FE	214	233	8.5	32	Y-CC
	EXP/FE	1.00	1.05	1.05	1.07	

Where; Py and Δy load and mid-span deflection at yielding of bottom steel rebars, Pu ultimate load, Δu mid-span deflection at ultimate state, Y-CC bottom steel yielding followed by concrete crushing at mid-span, SF-TC shear failure of top chord, DB-SF-TC FRP debonding followed by shear failure of top chord.

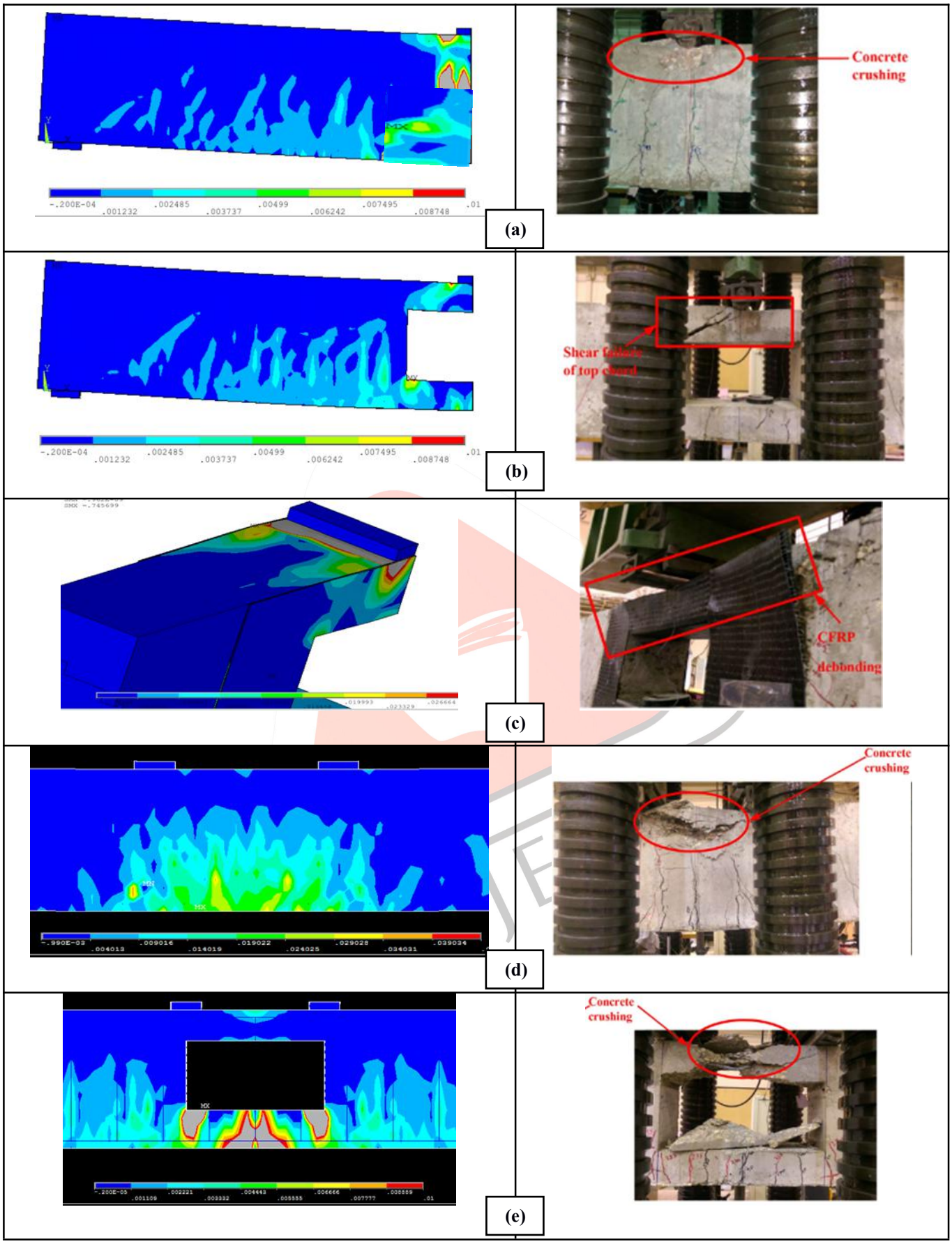

Fig. 13. Modes of failure for beams: **(a)** BU-N-CPL, **(b)** BU-4.0-CPL, **(c)** BS-4.0-CPL, **(d)** BU-N-4PB, and **(e)** BU-4.0-

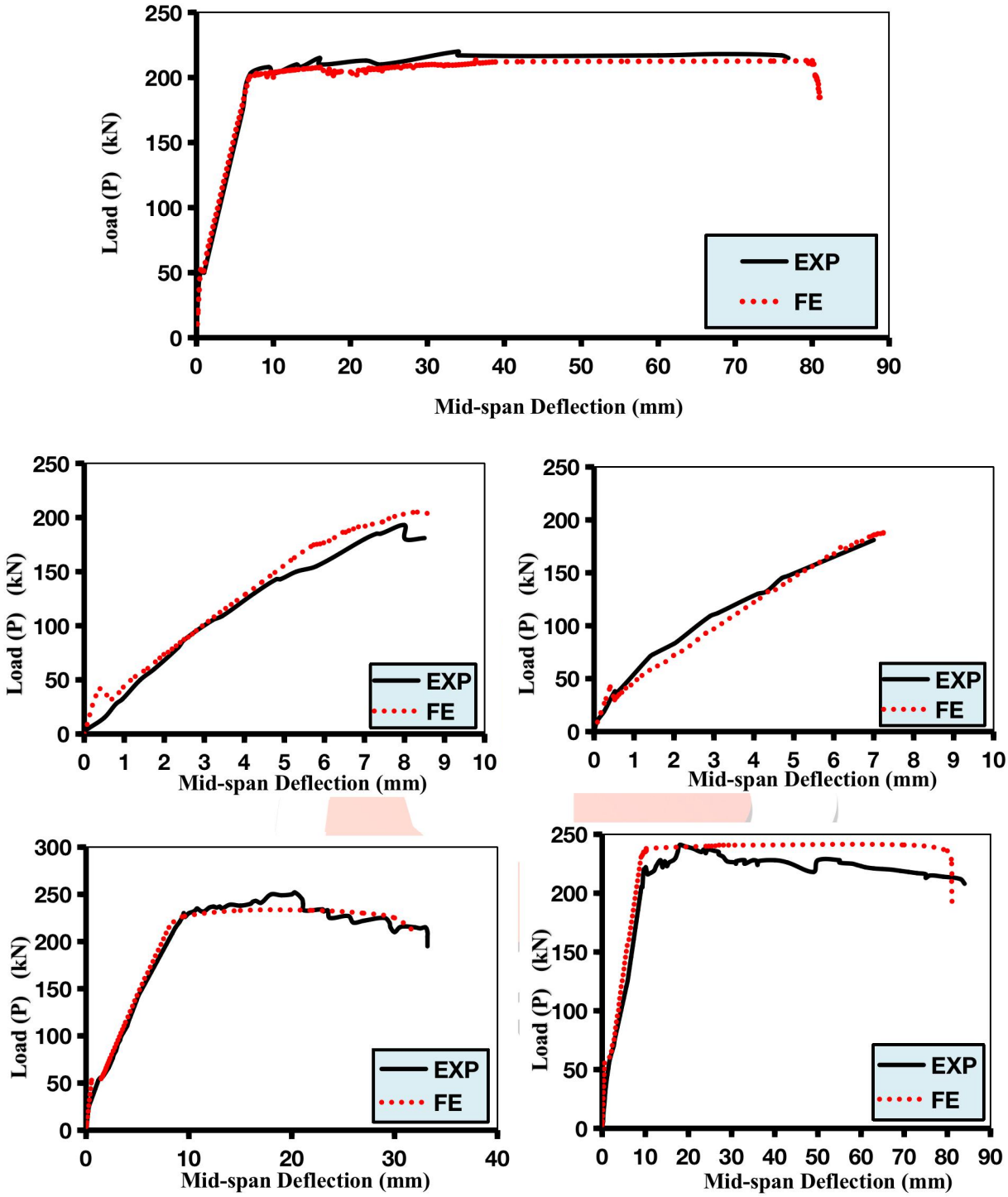

Table 4. FE load-deflection characteristics for the tested beams.

V. TEST RESULTS AND DISCUSSION

Cracking behavior and modes of failure

For beams with CPL, the results of analysis revealed that the failure of control beam BU-N-CPL with no opening started with the development of the flexural cracks that observed at the bottom edge of beam mid-span and the beam ultimately failed by crushing of concrete, and the cracking load was 21% of the ultimate load. For unstrengthened beams that have opening, diagonal cracks were first observed at the opposite corners of the opening and as the load was increased, these cracks widened and propagated both ways towards loading point. The cracking load was in the range of 13–20% of the ultimate load. For beam BU-N-CPL, with a small opening of 225x225 mm dimensions, the final failure was flexural failure of beam at opening region. But for the rest of unstrengthened beams with CPL the failure was a shear failure of the top chord of the opening. For strengthened beams, a diagonal shear crack was observed propagating at a small distance from the loading point all the way to the edge of the opening thereby shearing the top chord. However, before the final failure, debonding of the second CFRP layer externally bonded to the top chord was noticed at the location of the major shear crack.

For beams with 4PB, the final mode of failure of solid beam BU-N-APB was similar to that of control beam BU-N-CPL tested under center-point bending. The beam failed in flexure with the yielding of longitudinal rebars leading to the crushing

of concrete at the critical section. The cracking load for this solid beam was 24% of the ultimate load. For unstrengthened beam BU-4.0-4PB with opening and as a result of four-point bending setup, with two point loads applied at a distance of 450 mm from each other, the maximum bending moment was created within the section of the beam at the location of the opening. Failure of this beam was in flexure with cracks developing in tension zone and becoming wider as the load increased. Final failure was caused as a result of the top chord concrete crushing suddenly due to the presence of opening.

From **Table 4**, it can be seen that the cracking load of the CFRP-strengthened beams increased due to strengthening than unstrengthened beams have the same openings. the size of the opening and FRP strengthening had a great effect on the cracking load. The cracking load decreased as the opening size was increased and it increased at strengthened beams than those have the same opening. Crack patterns of some of the tested beams were shown in **Figs. 15**, **16**, **17**, **18** and **19**.

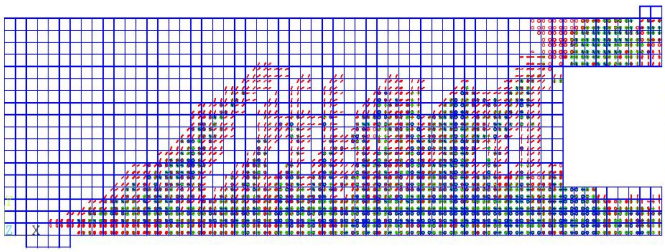

Fig. 15. Crack pattern of beam (BU-N-CPL)

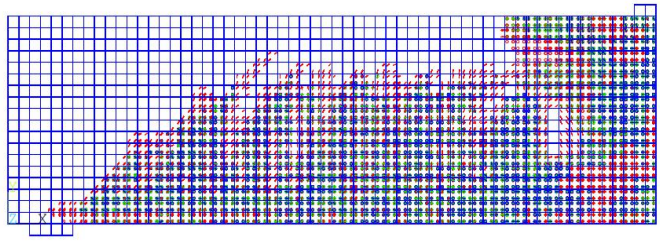

Fig. 16. Crack pattern of beam (BU-4.0-CPL)

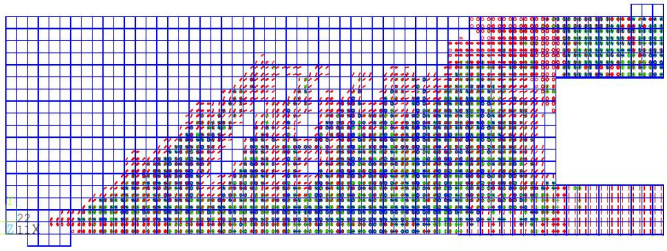

Fig. 17. Crack pattern of beam (BS-4.0-CPL)

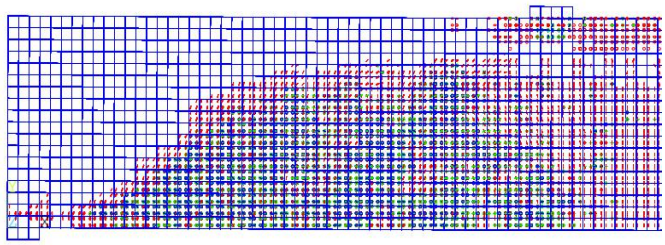

Fig. 18. Crack pattern of beam (BU-N-4PB)

G.	Beam ID.	Opening size (mm)		ℓ_o / h_c	External CFRP Strengthening	P_{cr} (KN)	P_y (KN)	P_u (KN)	Δ_y (mm)	Δ_u (mm)	Failure mode
		h_o	ℓ_o								
A	BU-N-CPL	--		0	No	45	173.3	212.8	6.9	81.2	Y-CC
	BU-2.0-CPL	225	225	2.0	No	41	153.2	200	6.7	38	FF-O
	BU-4.0-CPL	225	450	4.0	No	25.3	NY	187.7	NY	7.2	SF-TC
	BS-4.0-CPL	225	450	4.0	Yes	34	NY	204.8	NY	8.8	DB-SF-TC
	BU-6.0-CPL	225	675	6.0	No	19	NY	125	NY	5.6	SF-TC
	BS-6.0-CPL	225	675	6.0	Yes	23.3	NY	165.2	NY	6.7	DB-SF-TC
	BU-8.0-CPL	225	900	8.0	No	11.4	NY	86	NY	4	SF-TC
	BS-8.0-CPL	225	900	8.0	Yes	13	NY	135	NY	4.4	DB-SF-TC
B	BU-N-4PB	--		0	No	55	220	236	9.6	79.9	Y-CC
	BU-4.0-4PB	225	450	4.0	No	42.5	214	233	8.7	32	Y-CC
	BS-4.0-4PB	225	450	4.0	Yes	52	226	251	8.5	43.5	DB-FF-BC

Where; P_{cr} cracking load of concrete, FF-O flexural failure of beam at opening region, DB-FF-BC FRP debonding followed
by flexure failure of bottom chord.

Load-deflection curves

For the beams with center-point loading, load versus deflection curves are plotted in **Figs. 20**, **21**, **22** and **23**. As seen from Fig. 20, solid beam BU-N-CPL and beam BU-2.0-CPL, with unstrengthened opening 225x225 mm, showed the nearly

bilinear load-deflection response of under-reinforced concrete beams. For unstrengthened beam BU-4.0-CPL, with 225X450 mm opening the ultimate load was found to be 187.7 kN, which is about 88% of the ultimate load-carrying capacity of control solid beam
BU-N-CPL. Because of the single point load applied at beam mid-span, both maximum shear as well as maximum moment were created within the section of the beam at the location of the opening. The failure was sudden and as a result, the beam exhibited brittle behavior with small mid-span deflection. For CFRP strengthened beam BS-4.0-CPL, the ultimate load was 204.8 kN, which is about 9% increase over that of unstrengthened beam BU-4.0-CPL. This load is about 96% of the ultimate load of control solid beam BU-N-CPL. For unstrengthened beam BU-6.0-CPL, with 225X675 mm opening the ultimate load was found to be 125 kN, which is about 58% of the ultimate load-carrying capacity of control solid beam BU-N-CPL. For CFRP strengthened beam
BS-6.0-CPL, the ultimate load was 165.2 kN, which is about 32% increase over that of unstrengthened beam BU-6.0-CPL. This load is about 78% of the ultimate load of control solid beam BU-N-CPL. For unstrengthened beam BC-8.0-CPL, with large mid-span opening of 225x900 mm, the ultimate load was found to be 86 kN, which is about 40% of the ultimate load-carrying capacity of control solid beam BU-N-CPL. This load is considerably less compared to the control solid beam. This drop in the load is due to the larger size of the opening. Because of the large opening size, the top chord behaved as an independent beam supported between the two solid beam sections on either side of the opening. This had resulted in localized failure of the top chord with a small mid-span deflection of 4.1 mm at peak load, as seen in **Fig.23**. For CFRP strengthened beam BS-8.0-CPL, the ultimate load was 135 kN, which is about 57% increase over that of unstrengthened beam BU-8.0-CPL. This load is about 63% of the ultimate load of control solid beam BU-N-CPL. This revealed the ineptitude of scheme-1 in increasing the load capacity of RC beams with large opening located in the zone of high flexure with high shear.

For the three beams with 4-point bending, load versus deflection curves are plotted in **Fig. 24**. It is revealed that both beams BU-N-4PB, BU-4.0-4PB and BS-4.0-4PB had approximately the same behavior in terms of load-deflection characteristics, except that beams with opening failed at an earlier stage with low ultimate deflections of 32 mm for unstrengthened beam BU-4.0-4PB and 43.5 mm for strengthened beam BS-4.0-4PB compared with 79.9 mm for solid beam BU-N-4PB. The three beams showed nearly bilinear response of under-reinforced concrete beams. For unstrengthened beam BU-4.0-4PB, with 225X450 mm opening the ultimate load was found to be 214 kN, which is about 97% of the ultimate load-carrying capacity of control solid beam
BU-N-4PB. For CFRP strengthened beam BS-4.0-4PB, the ultimate load was 226 kN, which is about 7% increase over that of unstrengthened beam BU-4.0-4PB. This load is about 103% of the ultimate load of control solid beam BU-N-4PB.

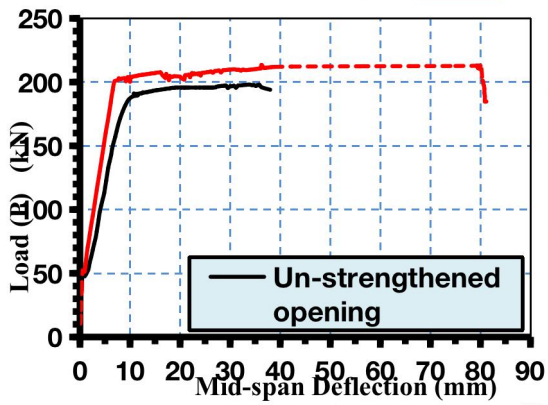

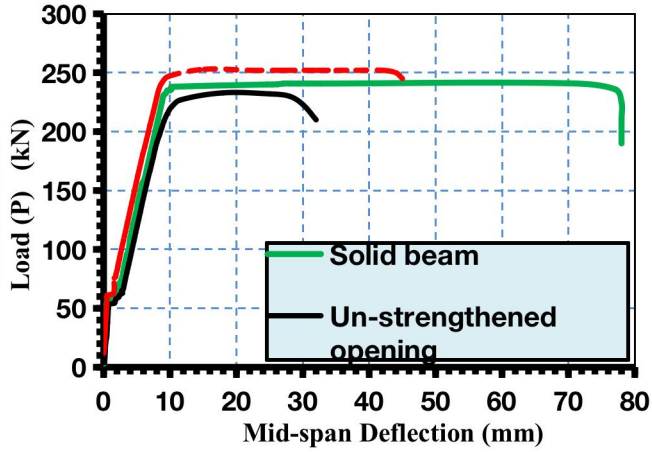

Fig. 20. Load-deflection curves for beams with CPL; solid beam and beam with opening 225x225 mm

Fig. 21. Load-deflection curves for beams with CPL having opening 225x450 mm.

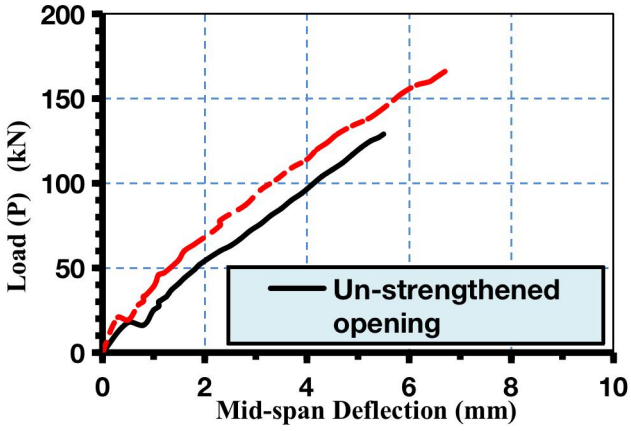

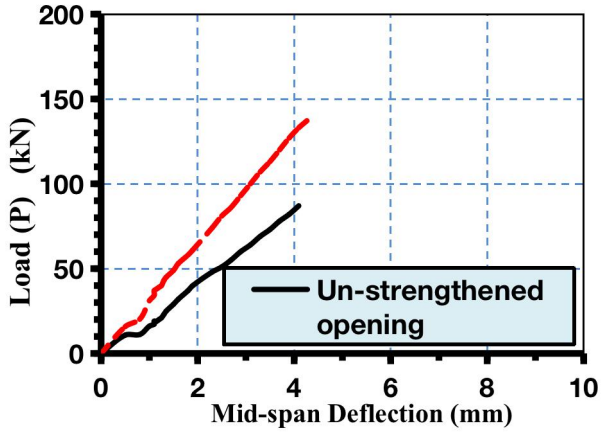

Fig. 22. Load-deflection curves for beam with CPL having opening 225x675 mm.

Fig. 23. Load-deflection curves for beam with CPL having opening 225x900 mm.

VI. CONCLUSIONS

This paper investigated effect of carbon fiber reinforced polymers (FRP) strengthening of RC beams with web opening in flexure zone using a three-dimensional finite element model using ANSYS V14 program. From the previous results and discussion, the following conclusions can be summarized: -

- The FE modeling used in this study was found appropriate in assessing the flexural strength of the unstrengthened as well as the FRP-strengthened RC beams with web openings in flexure zone. This demonstrates the validity of the modeling approach, which may be reliably used in future research on the use of FRP strengthening for RC structural members.
- For RC beams with opening in the pure flexure zone, the ultimate capacity is not influenced by the opening if the depth of the top chord is more than or equal to the depth of the concrete stress block at ultimate state. Hence, strengthening is not required for such cases.
- In cases where the depth of the top chord is less than the depth of the concrete stress block, strengthening may be needed to restore the beam strength. A further study is strongly recommended to come up with the most effective strengthening scheme in such cases.
- For RC beams with web openings located in the zone of high flexure with high shear (such as case of mid-span opening with center-point loading), reduction in strength due to opening is less than 10% when $\ell_o/h_c < 4$, where ℓ_o is the length of the opening and hc is the larger of h_b (depth of bottom chord) and h_t (depth of top chord). In this case, strengthening may not be needed.
- For beams with $4 \leq \ell_o/h_c < 8$, strengthening is required to restore he original beam strength. The proposed strengthening scheme of this study is recommended in this case.
- For beams with $\ell_o/h_c \geq 8$, strengthening with the proposed strengthening scheme of this study may not be efficient to fully restore the original beam strength.

REFERENCES

[1] T. Almusallam, Y. Al-Salloum, H. Elsanadedy, A. Alshenawy, and R. Iqbal, "Behavior of FRP-Strengthened RC Beams with Large Rectangular Web Openings in Flexure Zones: Experimental and Numerical Study," Int. J. Concr. Struct. Mater., vol. 12, no. 1, 2018.

[2] Arafa Mahmoud Ahmed, "Effect of opening on strength and serviceability of RC beams," Cairo university, 2010.

[3] M. A. Mansur, "Effect of Openings on the Behaviour and Strength of R / C Beams in Shear," Cem. Concr. Compos., vol. 20, pp. 477–486, 1998.

[4] W. Mansur, MA Tan, KH Wei, "Effects of creating an opening in existing beams," ACI Struct. J., vol. 96, no. 6, pp. 899–905, 1999.

[5] H. A. Abdalla, A. M. Torkey, H. A. Haggag, and A. F. Abu-Amira, "Design against cracking at openings in reinforced concrete beams strengthened with composite sheets," Compos. Struct., vol. 60, no. 2, pp. 197–204, 2003.

[6] T. El Maaddawy and S. Sherif, "FRP composites for shear strengthening of reinforced concrete deep beams with openings," Compos. Struct., vol. 89, no. 1, pp. 60–69, 2009.

[7] A. Pimanmas, "Strengthening R / C beams with opening by externally installed FRP rods: Behavior and analysis," Compos. Struct., vol. 92, no. 8, pp. 1957–1976, 2010.

[8] R. A. Hawileh, T. A. El-Maaddawy, and M. Z. Naser, "Nonlinear finite element modeling of concrete deep beams with openings strengthened with externally-bonded composites," Mater. Des., vol. 42, pp. 378–387, 2012.

[9] N. Z. Hassan, A. G. Sherif, and A. H. Zamarawy, "Finite element analysis of reinforced concrete beams with opening strengthened using FRP," Ain Shams Eng. J., vol. 8, no. 4, pp. 531–537, 2017.

[10] X. F. Nie, S. S. Zhang, J. G. Teng, and G. M. Chen, "Experimental study on RC T-section beams with an FRP-strengthened web opening," Compos. Struct., 2017.